Acta Pharmaceutica Sinica B 2020;10(12):2417–2432

Chinese Pharmaceutical Association
Institute of Materia Medica, Chinese Academy of Medical Sciences

Acta Pharmaceutica Sinica B

www.elsevier.com/locate/apsb
www.sciencedirect.com

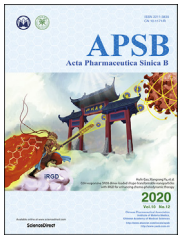

ORIGINAL ARTICLE

*Ii*WRKY34 positively regulates yield, lignan biosynthesis and stress tolerance in *Isatis indigotica*

Ying Xiao[a,†], Jingxian Feng[a,†], Qing Li[b], Yangyun Zhou[b], Qitao Bu[c], Junhui Zhou[d], Hexin Tan[c], Yingbo Yang[e], Lei Zhang[c,*], Wansheng Chen[a,b,*]

[a]*Research and Development Center of Chinese Medicine Resources and Biotechnology, Institute of Chinese Materia Medica, Shanghai University of Traditional Chinese Medicine, Shanghai 201203, China*
[b]*Department of Pharmacy, Changzheng Hospital, Naval Medical University (Second Military Medical University), Shanghai 200003, China*
[c]*Department of Pharmaceutical Botany, School of Pharmacy, Naval Medical University (Second Military Medical University), Shanghai 200433, China*
[d]*National Resource Center for Chinese Meteria Medica, China Academy of Chinese Medical Sciences, Beijing 100700, China*
[e]*Kanion Research Institute, Shanghai University of Traditional Chinese Medicine, Shanghai 201203, China*

Received 6 November 2019; received in revised form 14 November 2019; accepted 24 December 2019

KEY WORDS

Polyploidy vigor;
WRKY transcription factor;
Biomass production;
Lignan biosynthesis;
Stress tolerance

Abstract Yield potential, pharmaceutical compounds production and stress tolerance capacity are 3 classes of traits that determine the quality of medicinal plants. The autotetraploid *Isatis indigotica* has greater yield, higher bioactive lignan accumulation and enhanced stress tolerance compared with its diploid progenitor. Here we show that the transcription factor *Ii*WRKY34, with higher expression levels in tetraploid than in diploid *I. indigotica*, has large pleiotropic effects on an array of traits, including biomass growth rates, lignan biosynthesis, as well as salt and drought stress tolerance. Integrated analysis of transcriptome and metabolome profiling demonstrated that *IiWRKY34* expression had far-reaching consequences on both primary and secondary metabolism, reprograming carbon flux towards phenylpropanoids, such as lignans and flavonoids. Transcript–metabolite correlation analysis was applied to construct the regulatory network of *Ii*WRKY34 for lignan biosynthesis. One candidate target *Ii*4CL3, a key rate-limiting enzyme of lignan biosynthesis as indicated in our previous study, has been

*Corresponding author. Tel./fax: +86 21 51322403.
E-mail addresses: smmuipb@163.com (Lei Zhang), chenwansheng@smmu.edu.cn (Wansheng Chen).
†These authors made equal contributions to this work.
Peer review under responsibility of Institute of Materia Medica, Chinese Academy of Medical Sciences and Chinese Pharmaceutical Association.

https://doi.org/10.1016/j.apsb.2019.12.020

demonstrated to indeed be activated by *Ii*WRKY34. Collectively, the results indicate that the differentially expressed *Ii*WRKY34 has contributed significantly to the polyploidy vigor of *I. indigotica*, and manipulation of this gene will facilitate comprehensive improvements of *I. indigotica* herb.

1. Introduction

Polyploids often present novel phenotypes that are not found in their diploid progenitors, including enhanced organ size, biomass and stress tolerance, etc.[1] These traits often have some adaptive significance, allowing polyploids to increase their chances of being selected by nature, which we called "polyploidy vigor"[2]. The appearance of polyploidy vigor is demonstrated under complex genetic control, involving changes in gene expression through increased variation in dosage-regulated gene expression, epigenetic regulation and regulatory interactions[3]. Therefore, study on the gene expression related to the altered phenotype is crucial to clarify the underlying molecular mechanisms of polyploidy vigor, and will prompt the discovery of rational intervention strategies towards desired phenotypes.

Isatis indigotica Fort., belonging to the family Cruciferae, is a prevalent Chinese medicinal herb. The root of *I. indigotica* (Radix Isatidis), with Chinese name "Ban Lan Gen", is frequently used for the treatment of hepatitis, influenza and various kinds of inflammation[4]. Lignans, mainly including lariciresinol and its derivatives, have been identified as effective antiviral components of *I. indigotica*[5–7]. In our previous study, the tetraploid *I. indigotica* ($2n = 28$) with greater yield, higher lignans accumulation and enhanced stress resistance was obtained from its natural diploid progenitor ($2n = 14$)[8,9]. An *Arabidopsis thaliana* whole genome Affymetrix gene chip (ATH1)[10] was used to survey the variation of gene expression between tetraploid and diploid *I. indigotica*, and results revealed a coordinated induction and suppression of 715 and 251 ploidy-responsive genes in tetraploid *I. indigotica*, involving in various developmental, signal transduction, transcriptional regulation and metabolic pathways[11]. Some of them, such as a stomatal developmental gene *IiSDD1*[12], two signal transduction genes *IiCPK1*[13] and *IiCPK2*[14], and a lignan biosynthetic pathway gene *IiPAL*[15], have been characterized to explore their contribution to the favorable physiological consequences after polyploidization. More recently, transcriptomic analysis of diploid and tetraploid *I. indigotica* indicated that the differentially expressed genes (DEGs) were mainly involved in cell growth, cell wall organization, secondary metabolite biosynthesis, stress response and photosynthetic pathways[16]. Nevertheless, further studies are required to explore the mechanisms of the autotetraploidy vigor of *I. indigotica*.

Transcription factors (TFs) play essential roles in plants by controlling the expression of genes involved in various cellular processes, and are recognized to be particularly important in the process of crop domestication and are targets of molecular breeding of crops[17–19]. The comprehensive survey of global gene expression performed by ATH1 revealed eight TFs tend to be significantly higher in tetraploid than in diploid *I. indigotica*, and among them there are 4 *WRKY* genes[11]. Since the physiological role of WRKY TFs are widely related to diverse developmental processes, stress responses, and specialized metabolism[20], we reason that their expression variation in diploid and tetraploid *I. indigotica* might associate with altered phenotypes.

In the present study, a total of 64 *IiWRKY* genes (*IiWRKY1-64*) were first identified in *I. indigotica* transcriptome. In particular, *IiWRKY34* expression, significantly higher in tetraploids than in diploids, positively correlated with lariciresinol accumulation. Over-expression and RNAi analysis indicated that *Ii*WRKY34 is able to regulate lariciresinol biosynthesis, meanwhile, its upregulation improves root development, and enhances salt and drought stress tolerance. This study provides new insights into the genetic bases underlying the superiority of tetraploid *I. indigotica* compared to its diploid progenitor, as well as a potential target for genetic improvement of *I. indigotica* herb.

2. Materials and methods

2.1. Identification and characterization of IiWRKY genes

The homologous of *WRKYs* from the assembly of diploid *I. indigotica* transcriptome sequences[21] were searched using the BLASTx algorithm[22] from *A. thaliana* WRKYs (*At*WRKYs) and Chinese cabbage WRKYs (*Bra*WRKYs) respectively retrieved from The *Arabidopsis* Information Resource (http://www.arabidopsis.org/) and *Brassica* Database (BRAD, http://brassicadb.org/brad/). The Pfam database (pfam, http://pfam.janelia.org/)[23] and the Simple Modular Architecture Research Tool (SMART, http://smart.embl-heidelberg.de/)[24,25] were used to identify the putative WRKY proteins. The ProtParam tool (http://web.expasy.org/protparam) was further used to analyze the chemical and physical characteristics of these *Ii*WRKY proteins[26].

2.2. Bioinformatics analysis of IiWRKYs

The amino acid sequence alignments of *Ii*WRKYs alone, or along with *At*WRKYs were performed using CLUSTALX version 2.0.12[27]. Phylogenetic relationships were analyzed using the Neighbor-Joining method with pairwise deletion option in MEGA 5.05[28]. The putative polyploidy-responsive *Ii*WRKYs were identified through comparative analysis of orthologous genes between *I. indigotica* and *Arabidopsis*. According to the multiple sequence alignment and the previously reported classification of *At*WRKYs[29], the *Ii*WRKYs were assigned to different groups and subgroups. The possible conserved motifs were further detected by MEME[30]. *Ii*WRKY protein interactions were constructed by using STRING software (http://string-db.org/)[31].

2.3. Integrated analysis of IiWRKYs expression and lariciresinol accumulation

Tetraploid *I. indigotica* was generated followed the methods as described by Qiao[8] using *I. indigotica* ($2n = 14$) as the diploid donor. The supposed diploid and tetraploid plants were sampled to analyze ploidy levels using Quanta SC Flow Cytometer (Beckman Coulter, Brea, CA, USA)[16]. The hairy root culture was derived after infection of diploid and tetraploid *I. indigotica* plantlets with a Ri T-DNA bearing *Agrobacterium rhizogenes* bacterium (C58C1)[21]. Methyl jasmonate (MeJA, 0.5 μmol/L) treatment was performed on the day 18 post-inoculation, and the hairy roots were harvested at various time points (0, 1, 3, 6, 12 and 24 h). The harvested hairy roots, along with roots of diploid and autotetraploid *I. indigotica*, were used for RNA isolation and lariciresinol content determination.

Total RNAs were extracted using TRIzol Reagent (Thermo, Waltham, MA, USA), and the mRNAs were reversely transcribed by oligo dT to generate cDNA as a template. Real-time quantitative PCR (RT-qPCR) was used to analyze the transcripts of *IiWRKY33*, *IiWRKY34*, *IiWRKY48*, *IiWRKY49* and *IiWRKY50*. Gene-specific DNA primers for these *IiWRKYs* and the *I. indigotica* actin gene reported by Li et al.[32] were listed in Supporting Information Table S1. The RT-qPCR was performed according to manufacturer's instruction (Takara, Beijing, China). Quantification of the gene expression was done with comparative CT method. Three independent biological samples were analyzed. Experiments were performed in triplicate, and the results were represented by their mean ± standard deviation (SD).

Lariciresinol content was determined by triple-quadrupole mass spectrometer (Agilent 6410, Agilent, Santa Clara, CA, USA) following our previously published methods[33]. Multiple reaction monitoring mode was used for lariciresinol quantification with a selected transition of *m/z* 359 → 329. Lariciresinol standard was purchased from Sigma−Aldrich (St. Louis, MO, USA).

Correlations between *IiWRKYs* expression and lariciresinol accumulation were calculated by the Pearson correlation coefficient using *R* according to the co-occurrence principle between mRNA and metabolite levels[34].

2.4. Plasmid vector construction and transgenic hairy roots generation

The coding sequence of *IiWRKY34* was amplified by PCR using gene-specific primers *IiWRKY34*-F and *IiWRKY34*-R (Table S1). The PCR products were digested with *Bcl* I and *Spe* I, and ligated into plasmid PHB-flag to generate PHB-*IiWRKY34*-flag. For construction of the RNAi vector, an appropriate 351 bp fragment of *IiWRKY34* was amplified by PCR using primers *IiWRKY34*-s*Nco*I-a*Sal*I and *IiWRKY34*-s*Kpn*I-a*Xba*I (Table S1). The PCR products were then subcloned in opposite orientations on either side of the Pdk intron of the pCAMBIA1300-pHANNIBAL vector[35] to generate plasmids pCAMBIA1300-*IiWRKY34*. After sequencing confirmation, the above two plasmids, together with PHB-flag and pCAMBIA1300-pHANNIBAL as vector controls (control check, CK), were introduced separately into leaf explants of diploid *I. indigotica* by using *Agrobacterium tumefaciens* C58C1 strain and the generated hairy roots were screened using hygromycin. Hairy root lines generated through transformation with the blank C58C1 strain were used as wild-type (WT) control.

The hairy roots were cultured as described by Chen et al.[21] The fresh weight (determined as the difference between the whole flask with and without the harvested root tissues) was recorded at Day 9, 18, 27, 36, and 45 post-inoculation. The hairy roots harvested at the Day 45 were used for DNA extraction, RNA extraction, metabolite determination, microscopic analysis and phloroglucinol-HCl staining.

Genomic DNA was subjected for PCR analysis to detect exogenous *IiWRKY34* transformations using primers *IiWRKY34*-ovx-F and *IiWRKY34*-ovx-R (designed specifically to cover the gene sequence and the vector sequence, Table S1). For RNAi transgenic hairy roots, primers JDPDK-1F and JDPDKR (Table S1) were used to detect the inserted *IiWRKY34* fragment. The transformed status of hairy roots was also verified for the presence of genes *hpt* and *rolb* or *rolc*[36]. PCR-positive hairy roots were analyzed for *IiWRKY34* expression by using RT-qPCR analysis as described above.

The content of lignans was determined by LC−MS as described above. The selected transitions of *m/z* were 179 → 146 for conifer alcohol, 357 → 151 for pinoresinol, 359 → 329 for lariciresinol, 361 → 164 for secoisolariciresinol, 519 → 357 for pinoresinol 4-*O*-glucopuranoside, and 685 → 523 for secoisolariciresinol diglucoside, respectively. All the standards were purchased from Sigma−Aldrich.

Microscopic analysis of hairy roots was done essentially as described by De & Aronne[37]. Phloroglucinol-HCl staining was conducted to detect lignans, lignins, or wall-bound phenolics and derivatives, based on our previously published protocols[33].

2.5. Expression profile of IiWRKY34 in different tissues and under various treatments

Leaves of 2-month-old diploid *I. indigotica* seedlings were sprayed with salicylic acid (SA, 100 μmol/L), MeJA (100 μmol/L) or NaCl (200 mmol/L) and sampled at 0, 1, 3, 6, and 12 h after treatment. For drought treatment, the seedlings were subjected to 2.5% polyethylene glycol (PEG) for the indicated times. For UV-B treatment, the seedlings were exposed to 1500 J/m^2 UV-B light for 30 min, and then sampled at 0, 20, 40, 60 and 80 min during treatment, and at 30, 60, and 120 min post-treatment. The expression level of *IiWRKY34* in different tissues (roots, stems, leaves and flowers) and under various treatments was examined using RT-qPCR analysis as described above.

2.6. Determination of ROS level, proline content and total antioxidant capacity of transgenic hairy roots under stress treatments

The *IiWRKY34* overexpression and depression, along WT type hairy roots (20 g) were respectively subjected to salt and drought treatments by adding NaCl (75 mmol/L) and PEG (2.5%) into the liquid culture medium. After treatment for 5 days, reactive oxygen species (ROS) level was detected using the red fluorescence probe dihydroethidium (Vigorous, http://www.vigorousbiol.com/) following the methods as described by Wang et al.[38] Free proline content was determined as described by Bates et al.[39] Total antioxidant activities were evaluated for trolox equivalent antioxidant capacity (TEAC) using the methods as described by Zhang et al.[40]

2.7. Transcript profiling

The Illumina HiSeq2000 platform (San Diego, CA, USA) was used to investigate gene expression profile of the transgenic and WT hariy roots (3 groups × 5 biological replicates) harvested at the day 45 after inoculation. The raw reads were first generated using Solexa GA pipeline 1.6. After the removal of low-quality reads, the retained high-quality reads were mapped to previous annotation of *I. indigotica* transcriptome[21]. Tags were assigned to have significantly differential expression if they had a *P*-value of <0.05, a false discovery rate (FDR) of <0.05, and an estimated absolute fold-change >2 in sequence counts across libraries. These DEGs were further applied for Gene Ontology (GO) enrichment analysis[41] and Kyoto Encyclopedia of Genes and Genomes (KEGG) pathway enrichment analysis[42] to find out their biological implications or the involved pathway.

2.8. Untargeted metabolite profiling

Metabolites from 15 different samples (100 mg of fresh weight, 3 groups × 5 biological replicates) were extracted according to Lisec et al.[43] and determined by GC−TOF/MS (Agilent 7890, Agilent). The programs of temperature-rise was set as followed: 70 °C for 2 min, 10 °C/min rate up to 140 °C, 4 °C/min rate up to 240 °C, 10 °C/min rate up to 300 °C and staying at 300 °C for 8 min. Full-scan method with range from 50 to 600 (*m/z*) was used. The total mass of signal integration area was normalized for each sample, and the normalized data were imported into Simca-P software (version 11.5, http://www.umetrics.com/simca), employing PLS-DA model using the first principal component of VIP (variable importance in the projection) values (VIP>1) combined with Student's *t* test (*t*-test, $P < 0.05$) to find differentially expressed metabolites. The volcano plot was used to reveal significantly altered metabolite features *via* delineating a log transformation plot of the fold-change difference ($\log_2$ fold change value as *x*-axis) and the level of statistical significance ($-\log_{10}P$ value as the *y*-axis) of each metabolite. Metabolite alterations between *IiWRKY34*-OVX and *IiWRKY34*-RNAi lines were depicted in a map drawn according to KEGG pathway database.

2.9. Data mining

The assembly of transcriptome sequences was searched for *IiWRKYs* and the lariciresinol biosynthetic genes using our previously published protocols[33], and these gene expression patterns in different *IiWRKY34* transgenic lines (15 samples) were visualized with a heat map using the $\log_2$-transformed data in Multi-Experiment Viewer (version 4.9.0)[44]. Genes with different expression patterns were grouped through hierarchical clustering. Accordingly, a heat map showing lignans accumulation in different *IiWRKY34* transgenic lines was also constructed.

Correlation among *IiWRKY34*, lariciresinol biosynthetic genes and lignans were constructed using the Pearson correlation coefficient according to the co-occurrence principle[34]. The correlation network was generated using Cytoscape (version 3.6.0)[45].

2.10. EMSA

The *IiWRKY34* coding sequence was amplified using primers *IiWRKY34*-pET-F and *IiWRKY34*-pET-R (Table S1), and inserted into pET32a vector (Novagen, Darmstadt, Germany) between the sites NcoI and SacI to generate pET-*IiWRKY34* plasmid. This plasmid was then transformed into the *Escherichia coli* BL21 strain, and the recombinant protein was purified by using a His Spin Trap column (GE Healthcare, Buckinghamshire, UK). EMSA was performed using biotin-labelled probes and a Light-Shift chemiluminescent EMSA kit (Thermo, Chicago, IL, USA). To design biotin-labelled probes, a 1500-bp upstream region of *Ii4CL3* was amplified following the instructions of the Genome Walker Kit (Clontech, Mountain View, CA, USA), and analysed for the presence of W-boxes (C/T)TGAC (T/C). The biotin-labelled probes (Table S1) were synthesized by Sangon Biotech Company (Shanghai, China).

2.11. Dual luciferase assay

The coding sequence of *IiWRKY34* was subcloned into the PHB vector (Biovector, Beijing, China) to generate the effector, and the promoter of *Ii4CL3* was fused into the vector pGreenII 0800 (Biovector) to generate a reporter. The reporter and effector constructs were then separately transformed into *A. tumefaciens* strain GV3101. The bacterial cells were resuspended in MS medium with 10 mmol/L methylester sulfonate and 150 μmol/L acetosyringone to $OD_{600} = 0.6$ and then incubated at room temperature for 3 h. The bacteria-harboring constructs were infiltrated into tobacco leaves according to Zhang et al.[46] The leaves were collected after 48 h for dual-LUC assays using a Dual-Luciferase Reporter Assay System according to the manufacturer's instructions (Promega, Madison, WI, USA). Three independent biological replicates were measured for each sample.

2.12. Statistics

Experiments were performed in triplicate, and statistical analysis was performed using SPSS 22.0 software. Paired, two-tailed Student's *t*-test was used to compare group differences. *P*-values<0.05 were regarded as statistically significant.

2.13. Data availability

The nucleotides and amino acid sequences of *IiWRKYs* (*IiWRKY1* to *IiWRKY64*) are deposited in the GenBank databases under the accession numbers (MN480587 to MN480650). The raw RNA-seq read data are accessible through accession number PRJNA491805 (http://www.ncbi.nlm.nih.gov/sra/).

3. Results

3.1. Identification and characterization of WRKY genes in I. indigotica

A total of 64 putative *IiWRKY* genes (*IiWRKY1* to *IiWRKY64*) were identified (Supporting Information Table S2). The ORFs were extracted from the putative *IiWRKY* sequences, and then converted into amino acid sequences (Supporting Information Table S3). Detailed information about each *IiWRKY* is given in Table 1.

Sequence alignment of the unique DNA-binding domain, spanning approximately 60 amino acids of all 64 *Ii*WRKYs revealed that all *Ii*WRKYs contain the highly conserved DNA binding domain composed of the conserved WRKYGQK sequence followed by a C_2H_2- or C_2HC-type zinc finger motif

Table 1 Identification of *WRKY* genes in *I. indigotica.*

Group	Subgroup	Gene ID	Gene locus ID	CDS (bp)	ORF (aa)	Mass (kDa)	pI	Atortholog		
								*At*Gene ID	*At*Locus	Identity (%)
I		*IiWRKY3*	comp12944_c0_seq1	1443	480	52.36	5.47	*AtWRKY32*	AT4G30935.1	74.07
		IiWRKY5	comp14011_c0_seq1	594	197	22.08	8.86	*AtWRKY20*	AT4G26640.1	90.86
		IiWRKY14	comp22052_c1_seq1	717	238	26.16	9.30	*AtWRKY44*	AT2G37260.1	84.45
		IiWRKY17	comp22961_c0_seq1	1392	463	50.46	8.73	*AtWRKY58*	AT3G01080.1	76.33
		IiWRKY33	**comp27067_c0_seq1**	**1548**	**515**	**56.76**	**8.37**	***AtWRKY33***	**AT2G38470.1**	**84.95**
		IiWRKY36	comp27813_c0_seq2	972	323	36.24	9.45	*AtWRKY26*	AT5G07100.1	74.53
		IiWRKY37	comp27813_c0_seq4	375	124	14.46	9.56	*AtWRKY26*	AT5G07100.1	77.65
		IiWRKY48	**comp32055_c0_seq1**	**1065**	**354**	**39.73**	**7.70**	***AtWRKY25***	**AT2G30250.1**	**71.00**
		IiWRKY49	**comp32055_c0_seq2**	**1224**	**407**	**45.56**	**7.19**	***AtWRKY25***	**AT2G30250.1**	**84.54**
		IiWRKY53	comp32270_c3_seq7	1521	506	54.83	8.67	*AtWRKY4*	AT1G13960.1	89.17
		IiWRKY54	comp32270_c3_seq8	1548	515	56.23	6.98	*AtWRKY3*	AT2G03340.1	83.43
		IiWRKY60	comp34055_c0_seq1	1431	476	52.80	8.70	*AtWRKY1*	AT2G04880.2	76.72
II	**a**	***IiWRKY34***	**comp27256_c0_seq2_1**	**909**	**302**	**33.43**	**7.55**	***AtWRKY40***	**AT1G80840.1**	**88.12**
	a	*IiWRKY51*	comp32255_c0_seq1_1	762	253	28.16	8.80	*AtWRKY60*	AT2G25000.1	72.14
	a	*IiWRKY52*	comp32255_c0_seq2_2	729	242	26.81	8.61	*AtWRKY60*	AT2G25000.1	74.00
	b	*IiWRKY11*	comp19028_c0_seq1	1587	528	58.63	6.39	*AtWRKY61*	AT1G18860.1	77.91
	b	*IiWRKY13*	comp20394_c0_seq1	1368	455	50.41	6.79	*AtWRKY47*	AT4G01720.1	82.81
	b	*IiWRKY21*	comp26285_c0_seq1	1539	512	56.04	5.94	*AtWRKY42*	AT4G04450.1	80.63
	b	*IiWRKY31*	comp26827_c0_seq1	885	294	33.43	8.12	*AtWRKY9*	AT1G68150.1	73.73
	b	*IiWRKY39*	comp28388_c0_seq1	1173	390	43.18	6.17	*AtWRKY36*	AT1G69810.1	67.65
	b	*IiWRKY55*	comp32451_c1_seq1	1617	538	58.46	5.48	*AtWRKY31*	AT4G22070.1	88.27
	b	*IiWRKY61*	comp36248_c0_seq1	1728	575	62.32	8.81	*AtWRKY72*	AT5G15130.1	85.23
	c	*IiWRKY2*	comp12464_c0_seq1	972	323	36.56	5.94	*AtWRKY49*	AT5G43290.1	70.37
	c	*IiWRKY6*	comp14046_c0_seq1	1236	411	46.24	6.37	*AtWRKY48*	AT5G49520.1	81.88
	c	*IiWRKY10*	comp17362_c0_seq1	585	194	22.38	6.30	*AtWRKY59*	AT2G21900.1	78.71
	c	*IiWRKY15*	comp22285_c0_seq2	465	154	18.02	8.48	*AtWRKY8*	AT5G46350.1	83.77
	c	*IiWRKY19*	comp24875_c0_seq2	192	63	7.39	9.39	*AtWRKY50*	AT5G26170.1	93.65
	c	*IiWRKY22*	comp26365_c0_seq1	618	205	23.2	5.88	*AtWRKY51*	AT5G64810.1	85.50
	c	*IiWRKY23*	comp26532_c0_seq1	939	312	34.85	6.62	*AtWRKY28*	AT4G18170.1	83.85
	c	*IiWRKY24*	comp26532_c0_seq2	930	309	34.63	8.24	*AtWRKY28*	AT4G18170.1	66.87
	c	*IiWRKY25*	comp26532_c0_seq3	852	283	31.95	7.74	*AtWRKY71*	AT1G29860.1	79.79
	c	*IiWRKY26*	comp26532_c0_seq4	861	286	32.16	6.46	*AtWRKY71*	AT1G29860.1	64.86
	c	*IiWRKY28*	comp26776_c0_seq1	528	175	20.20	9.51	*AtWRKY57*	AT1G69310.1	90.12
	c	*IiWRKY29*	comp26776_c0_seq5	999	332	36.95	6.98	*AtWRKY57*	AT1G69310.1	78.98
	c	*IiWRKY30*	comp26776_c0_seq9	540	179	20.73	9.63	*AtWRKY57*	AT1G69310.1	90.00
	c	*IiWRKY32*	comp26972_c0_seq2	441	146	16.77	9.37	*AtWRKY75*	AT5G13080.1	85.81
	c	*IiWRKY35*	comp27574_c0_seq1	1113	370	41.52	7.32	*AtWRKY23*	AT2G47260.1	80.86
	c	*IiWRKY38*	comp27813_c0_seq7	576	191	21.52	7.00	*AtWRKY56*	AT1G64000.1	82.50
	c	*IiWRKY40*	comp28803_c0_seq1_1	519	172	19.82	8.97	*AtWRKY12*	AT2G44745.1	89.40
	c	*IiWRKY41*	comp28803_c0_seq2_2	399	132	15.51	9.30	*AtWRKY12*	AT2G44745.1	94.70
	c	*IiWRKY56*	comp32704_c0_seq5	432	143	16.51	9.01	*AtWRKY45*	AT3G01970.1	75.84
	d	*IiWRKY8*	comp16130_c0_seq1	1038	345	37.72	9.62	*AtWRKY11*	AT4G31550.2	82.61
	d	*IiWRKY45*	comp31187_c4_seq1	1041	346	38.24	9.75	*AtWRKY74*	AT5G28650.1	85.26
	d	*IiWRKY46*	comp31187_c4_seq3	996	331	36.74	9.51	*AtWRKY39*	AT3G04670.1	89.46
	d	*IiWRKY47*	comp31456_c3_seq4	588	195	21.83	9.44	*AtWRKY15*	AT2G23320.1	90.97
	d	***IiWRKY50***	**comp32075_c0_seq1**	**687**	**228**	**25.35**	**9.64**	***AtWRKY21***	**AT2G30590.1**	**84.65**
	d	*IiWRKY62*	comp37405_c0_seq1	1038	345	37.81	9.77	*AtWRKY7*	AT4G24240.1	77.93
	e	*IiWRKY7*	comp15334_c0_seq1	1269	422	45.77	5.17	*AtWRKY14*	AT1G30650.1	82.45
	e	*IiWRKY9*	comp17232_c0_seq1	900	299	32.35	6.39	*AtWRKY22*	AT4G01250.1	91.33
	e	*IiWRKY12*	comp19645_c0_seq1	870	289	31.64	5.60	*AtWRKY35*	AT2G34830.1	82.33
	e	*IiWRKY16*	comp22855_c0_seq1	828	275	30.59	5.09	*AtWRKY69*	AT3G58710.2	87.73
	e	*IiWRKY18*	comp24498_c0_seq1	777	258	28.91	5.52	*AtWRKY65*	AT1G29280.1	91.98
	e	*IiWRKY43*	comp30090_c0_seq1	552	183	20.37	4.57	*AtWRKY27*	AT5G52830.1	74.16
	e	*IiWRKY44*	comp30090_c0_seq3	1047	348	38.68	4.93	*AtWRKY27*	AT5G52830.1	73.86
	e	*IiWRKY64*	comp46853_c0_seq1	921	306	34.08	6.27	*AtWRKY29*	AT4G23550.1	86.18
III		*IiWRKY1*	comp7344_c0_seq2	786	261	29.77	5.66	*AtWRKY67*	AT1G66550.1	53.64
		IiWRKY4	comp13639_c0_seq2	894	297	33.32	6.01	*AtWRKY70*	AT3G56400.1	71.59
		IiWRKY20	comp25578_c2_seq1	870	289	32.90	5.71	*AtWRKY46*	AT2G46400.1	75.67
		IiWRKY27	comp26620_c0_seq1	1020	339	37.96	5.63	*AtWRKY54*	AT2G40750.1	74.65

(*continued on next page*)

Table 1 (*continued*)

Group	Subgroup	Gene ID	Gene locus ID	CDS (bp)	ORF (aa)	Mass (kDa)	pI	Atortholog		
								*At*Gene ID	*At*Locus	Identity (%)
		IiWRKY42	comp29870_c0_seq1	999	332	36.76	6.46	*AtWRKY41*	AT4G11070.1	69.37
		IiWRKY57	comp33243_c1_seq1	423	140	15.71	8.44	*AtWRKY55*	AT2G40740.1	65.44
		IiWRKY58	comp33243_c1_seq4	804	267	29.92	6.91	*AtWRKY55*	AT2G40740.1	52.28
		IiWRKY59	comp334956_c0_seq1	933	310	34.83	6.06	*AtWRKY30*	AT5G24110.1	75.56
		IiWRKY63	comp39251_c0_seq1	774	257	29.73	6.10	*AtWRKY62*	AT5G01900.1	80.15

Words in 'bold font' indicate the polyploidy-responsive *I. indigotica WRKY* genes and their corresponding information. CDS, coding sequence; ORF, open reading frame; bp, base pair; aa, amino acids; pI, isoelectric point.

(Supporting Information Fig. S1), which is the most prominent structural feature of WRKY protein[47]. These *Ii*WRKYs were classified into 3 large groups including groups I (12), II (43) and III (9) according to the structures of their WRKY domains, and the 43 group-II *Ii*WRKYs were further classified into 5 distinct subgroups (IIa−e) according to different conserved motif distributions (Table 1)[29]. Phylogenetic and structural analysis of *Ii*WRKYs were shown in Supporting Information Fig. S2. Moreover, a phylogenetic tree including 64 *Ii*WRKYs and 72 *At*WRKYs was shown in Supporting Information Fig. S3. Results indicated that *Ii*WRKYs evolved from group I to group II and finally to group III, paralleled with a WRKY evolutionary process observed in several other plant species[48−50].

3.2. *Identification of putative polyploidy-responsive IiWRKYs*

Generally speaking, proteins from the same taxonomic group probably have the same origin and exhibit relatively conserved function. Since *I. indigotica* and *Arabidopsis* belong to the same family (Cruciferae), we use *Arabidopsis* database to predict *Ii*WRKYs functions in the present study. Orthologous WRKYs between *I. indigotica* and *Arabidopsis* were summarized in Table 1.

In our previous survey of the gene expression difference between tetraploid and diploid *I. indigotica via* ATH1 by using 22,810 probe sets, the *WRKY* genes, corresponding to *Arabidopsis* probe sets *AtWRKY33* (At2g38470), *AtWRKY25* (At2g30250), *AtWRKY40* (At1g80840) and *AtWRKY21* (At2g30590), tend to be significantly higher in the tetraploids than in the diploids[11]. Here, the orthologous gene comparative analysis between *I. indigotica* and *Arabidopsis* clearly pinpointed the *IiWRKYs* with high homology to these *Arabidopsis* probe sets (Table 1), revealing in fact *IiWRKY33* (orthologous to *AtWRKY33*), *IiWRKY34* (orthologous to *AtWRKY40*), *IiWRKY48* (orthologous to *AtWRKY25*), *IiWRKY49* (orthologous to *AtWRKY25*) and *IiWRKY50* (orthologous to *AtWRKY21*) were precisely those polyploidy-responsive ones. *IiWRKY48* and *IiWRKY49* are paralogous genes, with 71% and 84.54% of identity to *AtWRKY25*, respectively.

An interaction network was constructed associated with WRKY *Arabidopsis* orthologs using *Ii*WRKYs. As shown in Fig. 1, many *Ii*WRKYs are involved in an interaction network that largely participate in plant defence regulatory pathways, as most factors affect plant stress responses, including STZ (salt tolerance zinc finger)[51], HD1 (involved in jasmonic acid and ethylene -dependent pathogen resistance)[52] and SIB1 (involved in responses to pathogen infection, jasmonic acid and SA stimulus)[53], etc. Interestingly, *Ii*WRKY33 (orthologous to *At*WRKY33), *Ii*WRKY34 (orthologous to *At*WRKY40), *Ii*WRKY48 (orthologous to *At*WRKY25) and *Ii*WRKY49 (orthologous to *At*WRKY25), which were predicted polyploidy-responsive, represent central nodes in the interaction networks that become activated by numerous elicitors and may integrate signaling from various stresses. However, *Ii*WRKY50, another polyploidy-induced member, was not integrated in the network.

3.3. *Integrated analysis of polyploidy-responsive IiWRKYs and lariciresinol*

The ploidy levels of diploid and tetraploid *I. indigotica* were confirmed *via* flow cytometric analysis as shown in Supporting Information Fig. S4. RT-qPCR analysis indicated that the transcript levels of *IiWRKY33*, *IiWRKY34*, *IiWRKY48*, *IiWRKY49* and *IiWRKY50* in roots of tetraploid *I. indigotica* were significantly higher than that of diploid ones ($P < 0.05$), and the fold changes were comparable with our microarray findings[11]. *IiWRKY33*, *IiWRKY34*, *IiWRKY48*, *IiWRKY49* and *IiWRKY50* were responsive to MeJA treatment in both diploid and tetraploid *I. indigotica* hairy roots, but with different patterns. It was obvious to note that *IiWRKY34* was more responsive to MeJA than other members, and its expression was dramatically up-regulated at 1 h post-treatment then lasted to the end of the experiment in both samples. It was interesting to note that the expression pattern of *IiWRKY33*, *IiWRKY34*, *IiWRKY48*, *IiWRKY49* and *IiWRKY50* in the induced hairy roots of tetraploid *I. indigotica* greatly differed from that in its original roots, suggesting the expression of these *IiWRKY* genes is under strict developmental and tissue-specific control. LC−MS analysis showed roots of tetraploid *I. indigotica* accumulated more lariciresinol than diploid progenitor ($P < 0.05$), consistent with our earlier finding that tetraploid *I. indigotica* exhibited higher antiviral effect compared with its diploid counterpart[9]. In addition, MeJA treatment greatly triggered lariciresinol production in both diploid and tetraploid *I. indigotica* hairy roots, but with different patterns that in diploids lariciresinol accumulation increased gradually and peaked at 12 h, whereas in tetraploids it decreased gradually until 3 h and then continuously increased from 3 to 24 h post treatment (Fig. 2A).

A correlation analysis between the above *IiWRKYs* and lariciresinol presented as a heat map (Fig. 2B) indicated that *IiWRKY34* was most highly correlated with lariciresinol with a correlation coefficient of 0.812, suggesting *Ii*WRKY34 probably positively regulated lariciresinol production.

3.4. *IiWRKY34 positively regulates lignan biosynthesis in I. indigotica hairy roots*

The role of *Ii*WRKY34 in lignan biosynthesis was investigated using a transgenic hairy root assay (Fig. 3). Two constructs (PHB-*IiWRKY34*-flag and pCAMBIA1300-*IiWRKY34*, Supporting

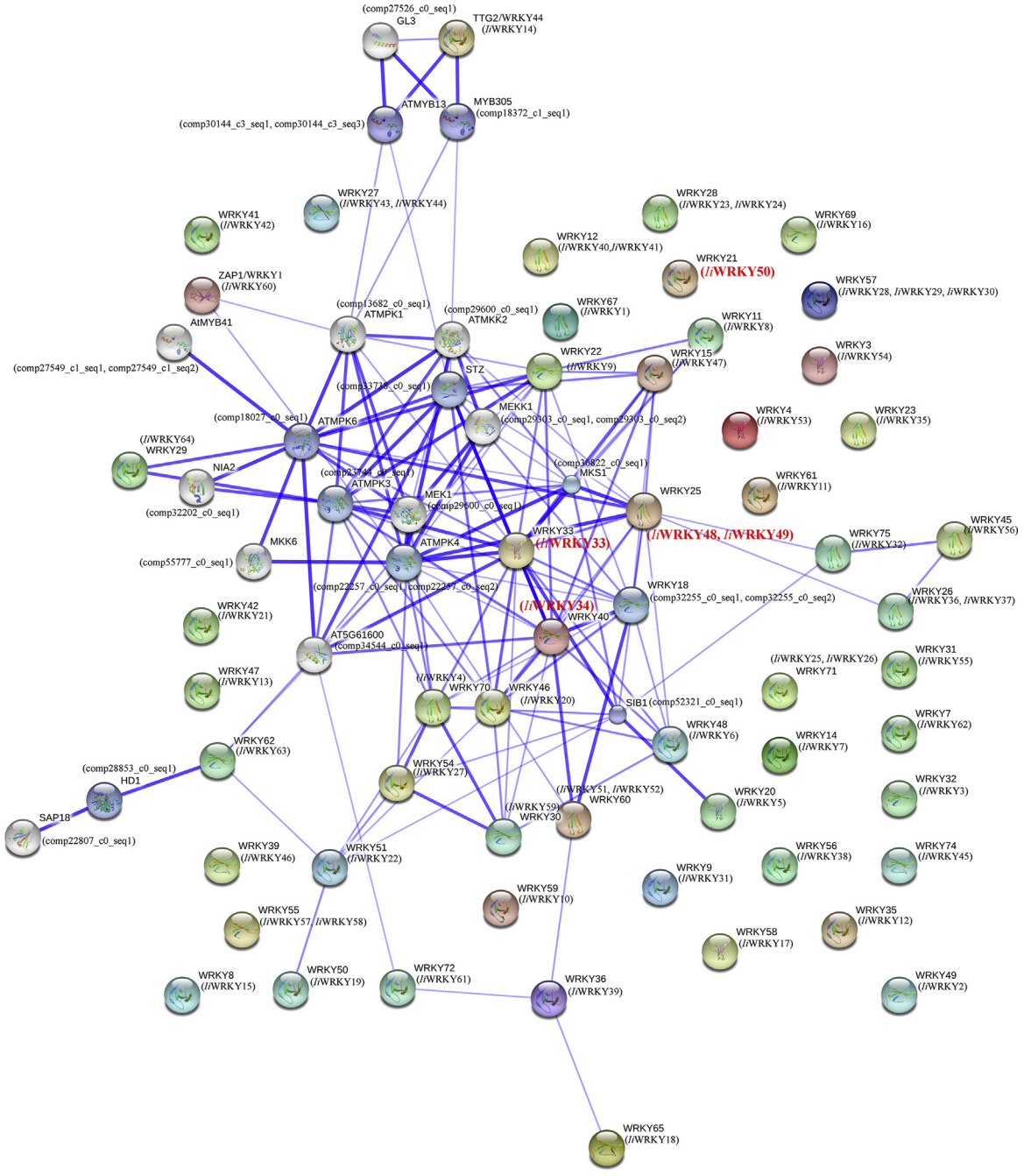

Figure 1 The interaction network of 64 *Ii*WRKY proteins identified in *I. indigotica* and related proteins in *Arabidopsis*. Stronger associations are represented by thicker lines. The polyploidy-responsive *Ii*WRKYs are denoted with red color.

Information Fig. S5) were generated for over-expression and RNA interference analysis (*IiWRKY34*-OVX and *IiWRKY34*-RNAi), respectively. The transformants were identified by PCR analysis: all the hairy roots contained the *rolb* or *rolc* gene, which indicated successful transformation of pRiA4[36]. The hygromycin resistance gene *hpt* was detected in both transgenic and CK lines. In addition, transgenic lines also contained *IiWRKY34*-specific fragments (Supporting Information Fig. S6).

RT-qPCR analysis indicated that *IiWRKY34* expression level was successfully regulated through genetic manipulation that transgenic roots overexpressing *IiWRKY34* showed a dramatic increase in *IiWRKY34* expression, whereas *IiWRKY34*-RNAi roots showed a significant reduction compared with WT and CK ($P < 0.05$, Fig. 3G). It was interesting to note *IiWRKY34*-OVX roots grew fast and vigorously with thick branches whereas *IiWRKY34*-RNAi roots grew slowly with slender branches (Fig. 3A). At the Day 45 after inoculation, the biomass of *IiWRKY34*-OVX and *IiWRKY34*-RNAi roots were approximately 3.7- and 0.3-fold of WT respectively, and no significant difference was detected between WT and CK (PHB, P1300) lines during the whole hairy root culture period (Fig. 3F). The morphology of different transgenic roots at the Day 45 was shown in Fig. 3B, and these roots were used to microscopic analysis and phloroglucinol-HCl staining. Microscopic analysis showed that when compared

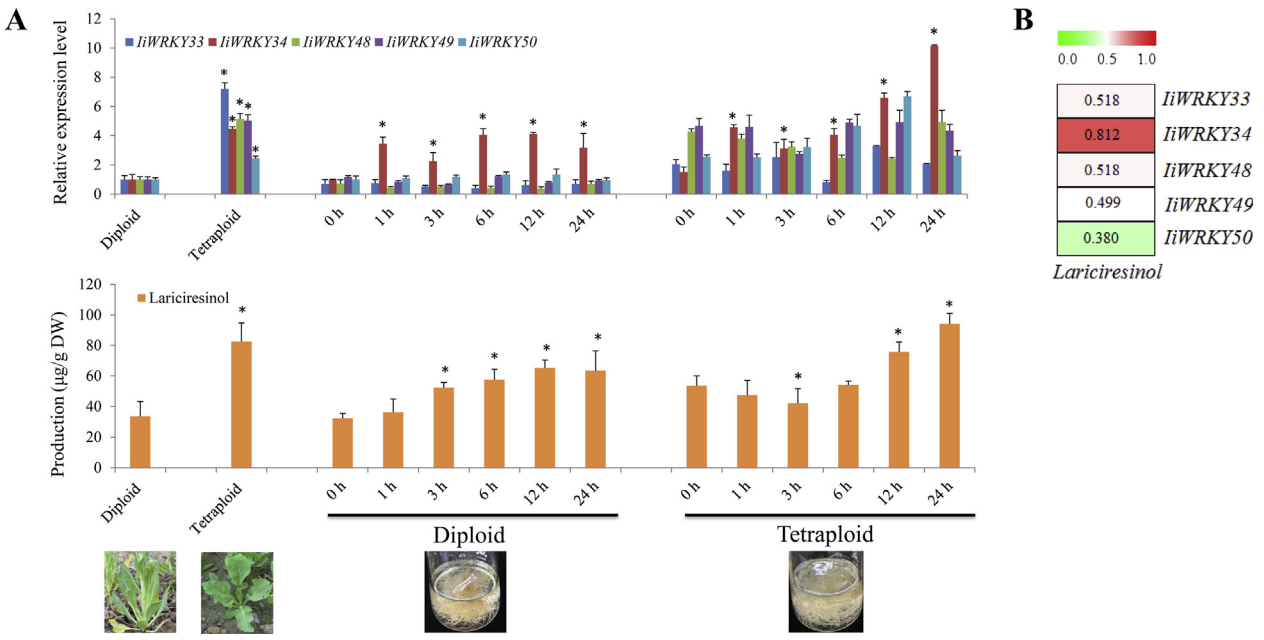

Figure 2 Integrated analysis of *IiWRKYs* expression and lariciresinol production. (A) *IiWRKY33*, *IiWRKY34*, *IiWRKY48*, *IiWRKY49* and *IiWRKY50* expression and lariciresinol production in response to autopolyploidy as well as MeJA treatment. Quantitative PCR analysis showing *IiWRKY33*, *IiWRKY34*, *IiWRKY48*, *IiWRKY49* and *IiWRKY50* expression relative to the control lines (diploid *I. indigotica*) set at 1. Data were expressed as means±SD ($n=3$). Asterisks represent significant difference at 0.05 level by Student's *t*-test. (B) Heat map showing *IiWRKY*−lignan correlation coefficients.

with WT and CK controls, the interfascicular fibers and xylem cells of *IiWRKY34*-OVX roots were relatively compacted with a higher lignification level, on the contrary those of *IiWRKY34*-RNAi counterparts were dispersed and had a lower lignification level (Fig. 3C). Phloroglucinol-HCl staining showed *IiWRKY34*-OVX roots presented a violet-red colour, whereas *IiWRKY34*-RNAi counterparts presented a weaker browning compared with WT and CK (Fig. 3D). Similar color was also found in their corresponding eluents (Fig. 3E). These results indicate that *Ii*WRKY34 positively improves the accumulation of lignans, lignins, and/or wall-bound phenolics and derivatives[54].

To test whether *Ii*WRKY34 positively improves the pharmaceutically important lignans, 6 compounds involved in lariciresinol biosynthetic pathway (Fig. 3H) were determined by LC−MS. Results showed that overexpression of *IiWRKY34* dramatically enhanced the production of the 6 lignans, and line OVX-4, with the highest *IiWRKY34* expression (20-fold of WT, Fig. 3G), produced the most abundant conifer alcohol (82.8 μg/g DW), pinoresinol (14.9 μg/g DW), lariciresinol (400.4 μg/g DW), secoisolariciresinol (184.5 μg/g DW), and secoisolariciresinol diglucoside (31.1 μg/g DW), which were ∼6.7-, 2.5-, 7.6-, 14.1- and 16.4-fold more than in WT, respectively. In contrast, RNAi suppression of *IiWRKY34* decreased the production of conifer alcohol, lariciresinol, secoisolariciresinol, and pinoresinol 4-*O*-glucopuranoside with different degrees. There was no significant difference in lignan content between CK and WT lines (Fig. 3I).

3.5. IiWRKY34 positively improves salt and drought stress tolerance in I. indigotica hairy roots

Expression of *IiWRKY34* was examined in various organs of 2-month-old *I. indigotica* seedlings, result showed that it was abundantly expressed in roots, stems and leaves, but only slightly expressed in flowers. *IiWRKY34* responded to drought, salt, SA, MeJA and UV-B treatments, but with different patterns of variation. After drought and salt treatment, the expression level of *IiWRKY34* increased gradually and reached a maximum at 6 h after treatment, which was approximately 7.3- and 24.2-fold, respectively, higher than that before treatment. When *I. indigotica* was treated with SA, *IiWRKY34* expression increased sharply at 1 h and peaked at 6 h (29.1-fold of that before treatment). Paralleled with MeJA-treated *I. indigotica* hairy roots (Fig. 2A), *IiWRKY34* expression in *I. indigotica* seedlings was induced by MeJA at 1 h (28.0-fold of that before treatment) post-treatment but decreased at 3 h, and then gradually increased afterward. For UV-B treatment, *IiWRKY34* expression gradually increased until 60 min and decreased at 80 min under UV-B, but its expression then increased after UV-B was turned off, and the expression level at 120 min achieved approximate 31.6-fold of that before treatment (Supporting Information Fig. S7). These results indicate that *IiWRKY34* can be significantly induced when subjected to environment stresses, which is in agreement with that *Ii*WRKY34 is involved in plant defence regulatory pathways as indicated in Fig. 1.

Both bioinformatics analysis (Fig. 1) and stress induction (Fig. S7) suggested a role of *Ii*WRKY34 in stress response. Thus, its capacity for stress tolerance was further investigated using transgenic hairy roots. Results showed *IiWRKY34* expression indeed could positively improve salt and drought stress tolerance. As shown in Fig. 4A, after 5 days of salt or drought treatment, both WT and *IiWRKY34*-OVX roots grew well as normal, but *IiWRKY34*-RNAi counterparts showed an early senescence phenotype with severe growth retardation compared with that without treatment (CK).

The intracellular ROS level in the WT and transgenic hairy roots was tested by fluorescence staining. Under normal conditions (CK), *IiWRKY34*-OVX root tips displayed a lower level of ROS whereas *IiWRKY34*-RNAi displayed a relatively higher level

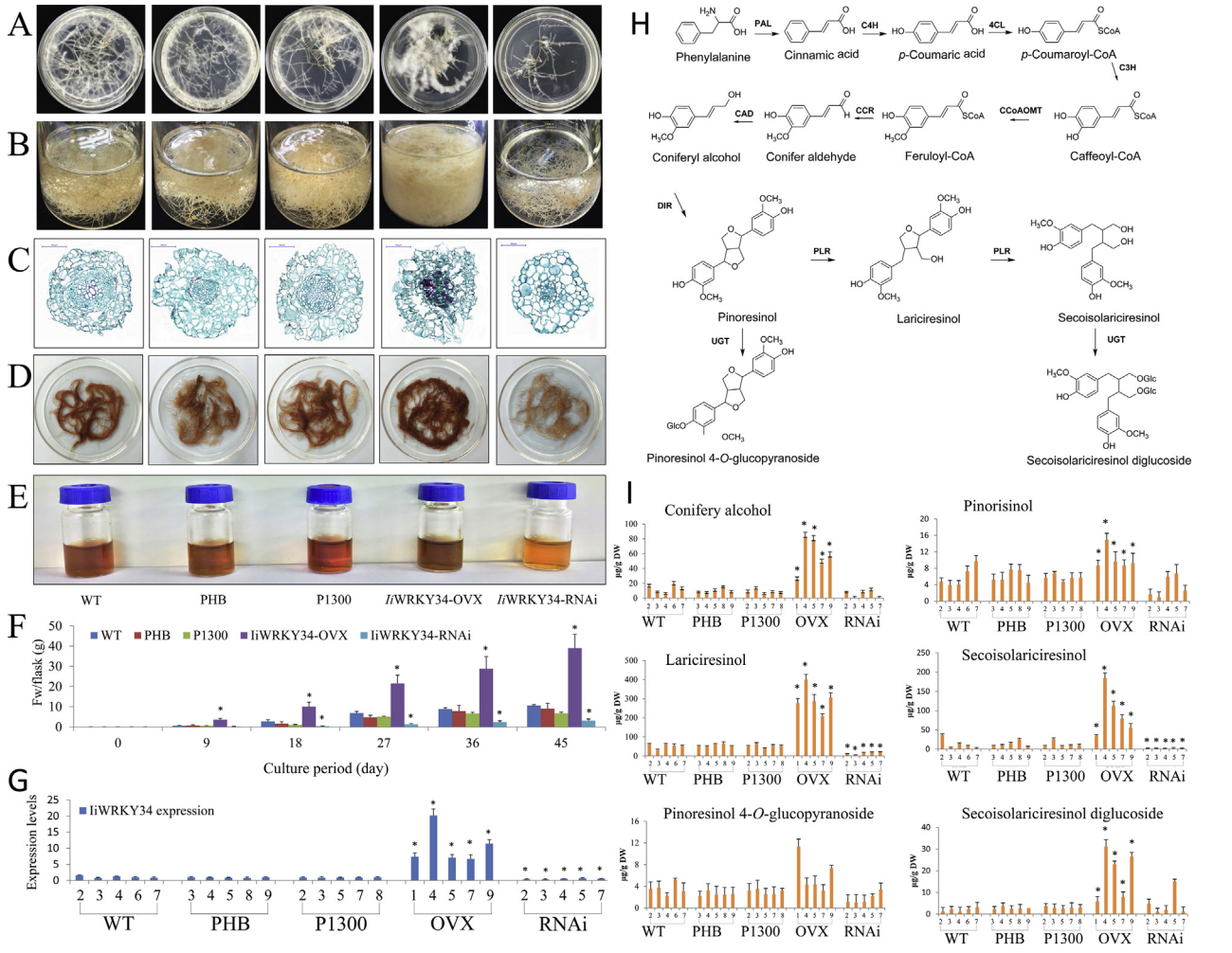

Figure 3 Phenotype analysis of *IiWRKY34* transgenic hairy roots. Phenotype of developed root lines on solid medium for 20 days (A), and their corresponding root culture in liquid medium for 45 days (B). (C) Cross sections of hairy roots stained with safranin O/fast green FCF. Bar = 100 μm. Phenotype (D) and eluents (E) of hairy roots after phloroglucinol-HCl staining. (F) Biomass accumulation during the culture period. *IiWRKY34* transcript expression (G) and lignan content (I) in different lines. Quantitative PCR analysis showing *IiWRKY34* expression relative to the wild-type lines (WT-2) set at 1. (H) lignan biosynthetic pathway. Data were expressed as means±SD ($n = 3$). Asterisks represent significant difference at 0.05 level by Student's *t*-test.

compared to WT. After salt or drought treatment, ROS accumulation enhanced in both WT and RNAi roots (especially in RNAi ones), while its accumulation in *IiWRKY34*-OVX roots still stayed at a low level as that in CK (Fig. 4B). These results imply that *Ii*WRKY34 may reduce the ROS level to confer salinity and drought stress tolerance.

Since proline accumulation is widely recognized as a sign of stress tolerance in plants[55], we examined whether the proline content in transgenic hairy roots was altered. Under salt or drought stress condition, both WT and *IiWRKY34*-OVX lines accumulated more proline than CK, and the proline content of *IiWRKY34*-OVX lines was much higher than that of WT. In contrast, the proline accumulation in *IiWRKY34*-RNAi lines was significantly decreased after salt treatment ($P < 0.05$), and remained approximately constant after drought condition (Fig. 4C). These results indicate that *Ii*WRKY34 may enhance salt and drought stress tolerance by promoting proline production.

Moreover, we measured TEAC to investigate the physiological effects of transgenic hairy roots. Compared with WT, *IiWRKY34*-OVX lines showed an approximate 1.5-fold increase in TEAC level, whereas *IiWRKY34*-RNAi showed a reduction by 1-s. After salt and drought treatment, the TEAC level of both WT and *IiWRKY34*-RNAi lines significantly decreased ($P < 0.05$), but that of *IiWRKY34*-OVX was barely changed (Fig. 4D). This result indicates *Ii*WRKY34 may maintain total antioxidant capacity to confer stress tolerance.

3.6. Gene expression profiles of transgenic I. indigotica hairy roots

Totally, 144,731 isogenes were identified by assembly. Differences in gene expression of the 3 groups (*IiWRKY34*-OVX, *IiWRKY34*-RNAi and WT hairy roots, 5 lines in each group) were shown in Fig. 5. Gene expression from individual groups showed a distinct sample separation (Fig. 5A), and a larger variation was found between *IiWRKY34*-OVX and *IiWRKY34*-RNAi lines compared with other pairwise samples that a total of 15,178 unigenes showed differential expression containing up-regulated and down-regulated ones (Fig. 5B). GO annotations indicated that these DEGs distributed in biological process, cellular component and molecular function categories with distinct patterns (Supporting Information Fig. S8). KEGG pathway enrichment analysis

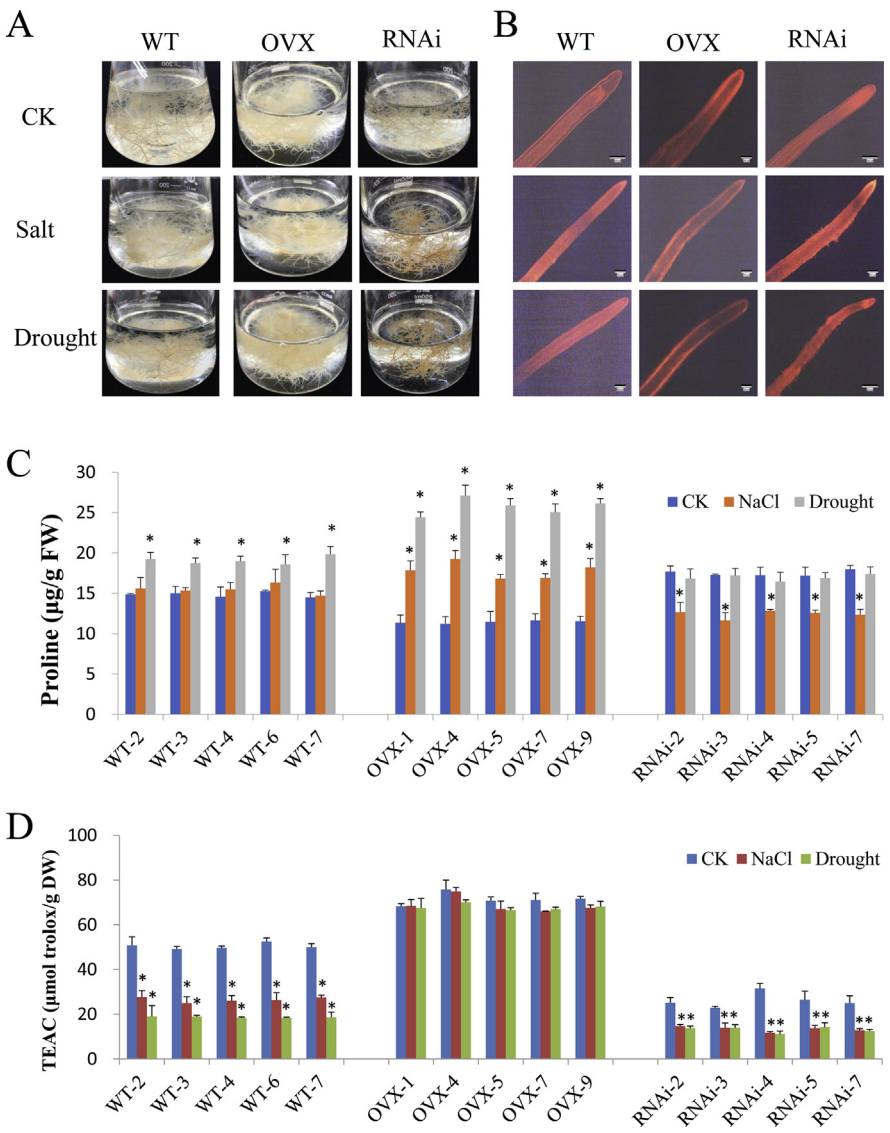

Figure 4 Performance of *IiWRKY34* transgenic hairy roots under salt and drought stresses. (A) Growth of transgenic hairy roots in 75 mmol/L NaCl, 2.5% PEG or liquid culture medium only for 5 days. ROS level (B), proline content (C) and trolox equivalent antioxidant activities (D) in different lines. The untreated wild-type hairy roots were designated as the control. Data were expressed as means±SD ($n=3$). Asterisks represent significant difference at 0.05 level by Student's *t*-test.

indicated that these DEGs were involved in biosynthesis of amino acids, carbon metabolism and phenylpropanoid, etc. The top 10 enriched pathways *via* pairwise contrasts presented in Fig. 5C distinguished a prominent variation between *IiWRKY34*-OVX and *IiWRKY34*-RNAi samples, and there were a total of 60 DEGs (17%) involved in phenylpropanoid biosynthesis.

The transcript levels of 64 *IiWRKY* in WT, *IiWRKY34*-OVX and *IiWRKY34*-RNAi hairy roots were presented as a heat map in Fig. 5D. As expected, *IiWRKY34* expression in *IiWRKY34*-OVX lines was higher than WT, whereas lower in *IiWRKY34*-RNAi counterparts, and the fold changes were paralleled well with that examined by RT-qPCR (Fig. 3G), indicating that the RNA-Seq expression profile is robust and gene expression level obtained from this database is reliable. It was interesting to note that *IiWRKY33*, *IiWRKY48* and *IiWRKY49*, which were found highly responsive to autopolyploidy (Fig. 2A), displayed a similar expression pattern with *IiWRKY34* and they grouped together, indicating they may associate with each other in some manners.

3.7. *Metabolite profiling of transgenic I. indigotica hairy roots*

To assess the impact of *Ii*WRKY34 on the metabolic shifts, nontargeted metabolic profiling was performed using GC−TOF/MS. Totally, 662 independent analytes were obtained from 15 samples. Differentially expressed metabolites (VIP>1, $P < 0.05$) in the 3 groups (*IiWRKY34*-OVX, *IiWRKY34*-RNAi and WT hairy roots, 5 lines in each group) were shown in Fig. 6. Similar with gene expression profiles (Fig. 5A), metabolite accumulation from individual groups also showed a distinct sample separation (Fig. 6A). Variation between *IiWRKY34*-OVX and *IiWRKY34*-RNAi lines was more significant than that between other pairwise samples, there were 113 and 52 metabolites found decreased and enhanced in abundances for *IiWRKY34*-OVX *versus* *IiWRKY34*-RNAi samples, respectively (Fig. 6B and Supporting Information Table S4). Generation of volcano plots further visualized the significantly altered metabolite features in *IiWRKY34*-OVX, *IiWRKY34*-RNAi and WT hairy roots (Fig. 6C).

To integrate both primary and secondary metabolism that had been modified by *IiWRKY34* expression, we used a pathway scheme to summarize the metabolic changes (VIP>1, $P < 0.05$) in *IiWRKY34*-OVX compared with *IiWRKY34*-RNAi roots. As shown in Fig. 6D, there were significantly higher amounts of phenylpropanoids such as flavonoids and lignans, whereas the basic sugar and the products of the TCA cycle, were reduced significantly, indicating that *Ii*WRKY34 appeared to reprogram primary metabolism, driving carbon flux towards specific secondary metabolism.

3.8. *Regulatory network of IiWRKY34 for lignan biosynthesis*

Metabolic analysis revealed that *IiWRKY34* positively regulated lignans production. To have a systematic view on the variation of lignan biosynthesis pathway, we examined abundances of 37 transcripts coding 9 catalytic genes (Supporting Information Tables S5) and 6 metabolites involved in lariciresinol biosynthesis in WT, *IiWRKY34*-OVX and *IiWRKY34*-RNAi hairy roots (5 lines in each group). The RNA-Seq expression profile indicated that lariciresinol biosynthetic genes responded to *IiWRKY34* transgene with various patterns (Fig. 7A). The accumulation levels of six lignans (Fig. 3I) were normalized and presented as a heat map in Fig. 7B. Correlation coefficient cut-off values were applied to construct *IiWRKY34*-pathway genes−lignans correlation networks. Fig. 7C presents one example with a cut-off $R > 0.5$: a total of 11 pathway genes are correlated with *IiWRKY34* and at least one lignan, indicating *Ii*WRKY34 may improve lignan biosynthesis by modulating these lignan biosynthetic genes. Among these genes, one *Ii4CL* family member *Ii4CL3* has been demonstrated as a key rate-limiting enzyme of lariciresinol production, severing as a hub gene of lignan regulatory network in our earlier study[56]. In order to test whether *Ii*WRKY34 regulate lignan by direct interacting with *Ii*4CL3, EMSA was performed using *Ii*WRKY34 recombinant protein and the promoter of *Ii4CL3*. Result showed *Ii*WRKY34 indeed specifically bound to the W-box in the promoter region of *Ii4CL3*. There are two W-boxes in the 1500-bp *Ii4CL3* promoter region (Supporting Information Fig. S9), and the biotin-modified probe representing the two TGAC core elements formed a DNA−protein complex with *Ii*WRKY34. Mutation of the two elements disrupted protein binding, and no retarded band representing complex formation was observed in the binding assay (Fig. 7D). Dual luciferase assay was further used to investigate how *Ii*WRKY34 regulate *Ii4CL3* by direct binding to its promoter sequence (Fig. 7E). Result showed *Ii*WRKY34 activated the promoter of *Ii4CL3 in vivo*, as evidenced by a higher value of LUC/REN than the control (Fig. 7F), supporting the hypothesis that *Ii*WRKY34 interacts with the promoter of *Ii4CL3* and thus activates its transcription.

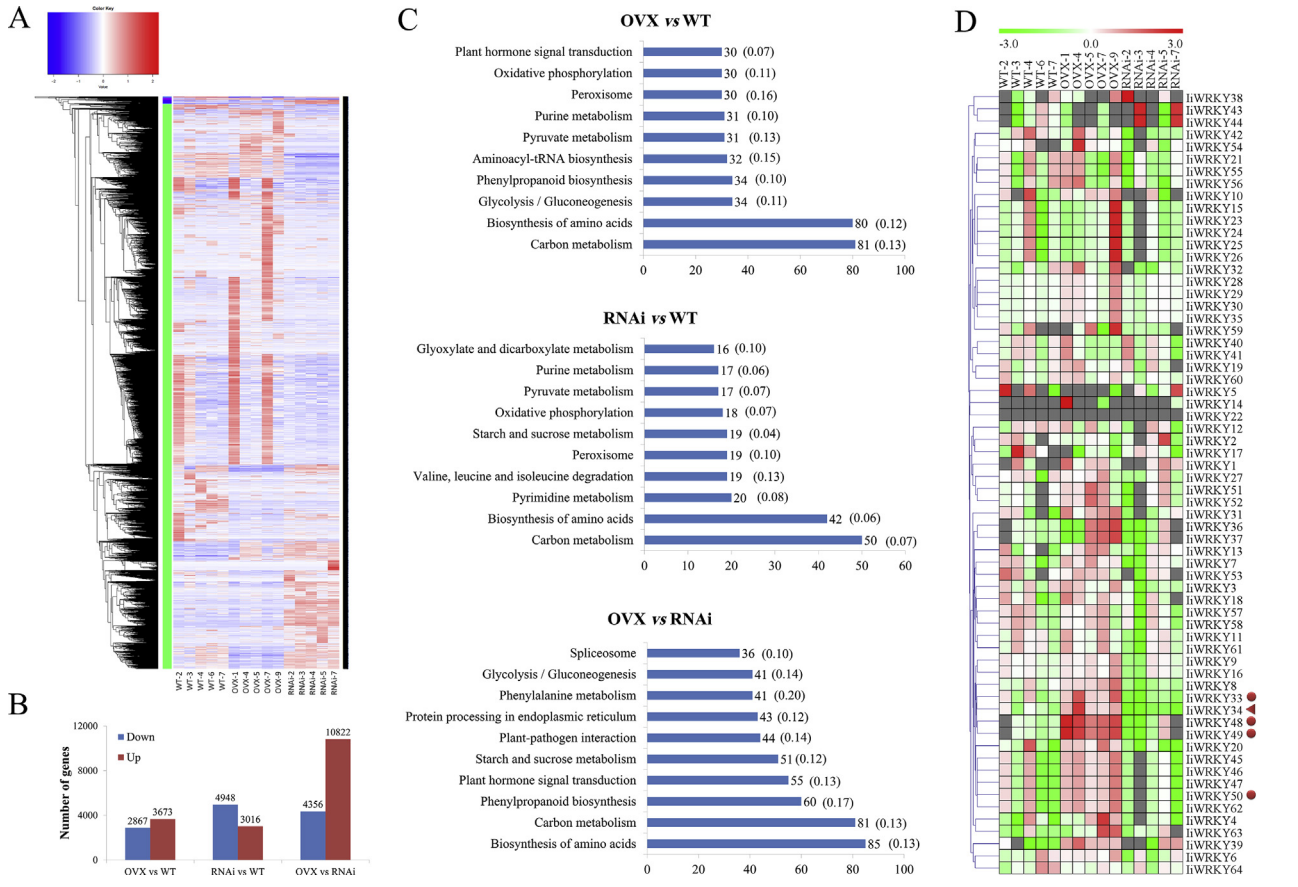

Figure 5 Gene expression profiles of *IiWRKY34* transgenic hairy roots. (A) Heat map showing DEGs in *IiWRKY34*-OVX, *IiWRKY34*-RNAi and WT lines. (B) Number of DEGs *via* pairwise contrasts of *IiWRKY34*-OVX, *IiWRKY34*-RNAi and WT roots with fold-change >2 and FDR <0.05. (C) Numbers of DEGs in the top ten enriched pathways. In parentheses: percentage of the total number of genes in the respective pathway. (D) Expression profiles of 64 *IiWRKY*s in different lines. *IiWRKY33*, *IiWRKY34*, *IiWRKY48*, *IiWRKY48* and *IiWRKY50* are highlighted with red markers.

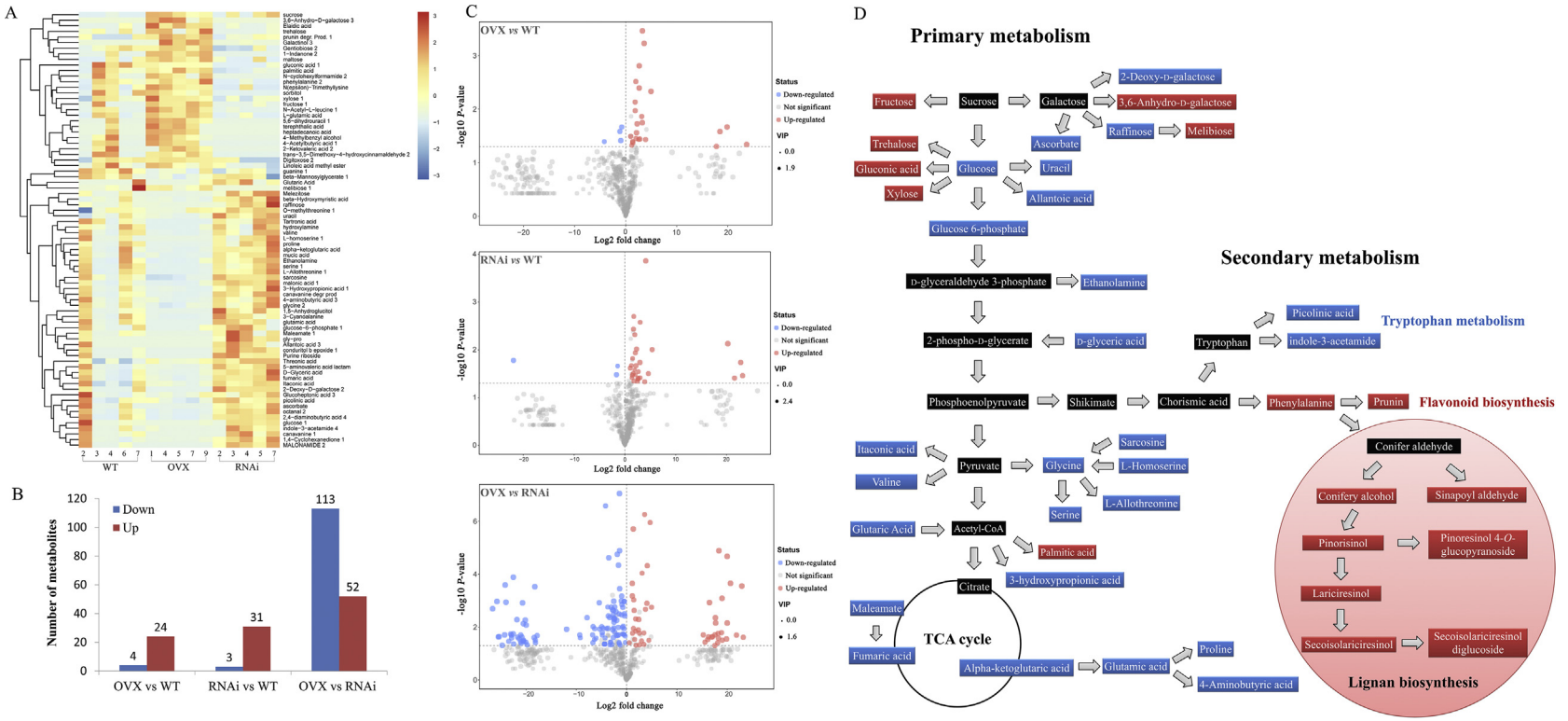

Figure 6 Metabolite profiling of *IiWRKY34* transgenic hairy roots. (A) Heat map showing differentially expressed metabolites of *IiWRKY34*-OVX, *IiWRKY34*-RNAi and WT lines. (B) Number of metabolites with significant changes in concentration (VIP>1, $P<0.05$) *via* pairwise contrasts. (C) Volcano plot of differentially expressed metabolites *via* pairwise contrasts. (D) Pathway scheme summarizing the metabolic changes in *IiWRKY34*-OVX compared with *IiWRKY34*-RNAi transgenic roots. Metabolites which changed significantly (VIP>1, $P<0.05$) are highlighted in red (for increased) and blue (for decreased), metabolites without significant changes are highlighted in black.

4. Discussion

Yield potential, medicinal compounds concentration and stress tolerance capacity are 3 classes of traits determining the quality of herbs. Tetraploid *I. indigotica* has been appealing to people because of its greater yield, higher bioactive compounds accumulation and enhanced stress tolerance compared to its diploid counterpart. Elucidation of the underlying molecular basis of the significantly qualitative difference is of great importance for the improvement of *I. indigotica*.

In the present study, *IiWRKY33*, *IiWRKY34*, *IiWRKY48*, *IiWRKY49* and *IiWRKY50*, which express especially higher in tetraploid *I. indigotica* than diploids, were proposed to be particularly important in the trait development seen in the tetraploids. An interaction network constructed using *Arabidopsis* database revealed *Ii*WRKY33, *Ii*WRKY34, *Ii*WRKY48 and *Ii*WRKY49 located as hub genes and associated with various defence regulatory pathways (Fig. 1), suggesting they might have contributed to the higher stress resistance of tetraploid *I. indigotica*. Previous reports of their *Arabidopsis* homologues *At*WRKY33 (orthologous to *Ii*WRKY33), *At*WRKY40 (orthologous to *Ii*WRKY34) and *At*WRKY25 (orthologous to *Ii*WRKY48 and *Ii*WRKY49) confirmed the reliability of this functional protein association network. For instance, overexpression of *At*WRKY25 and *At*WRKY33 increased salt tolerance and ABA sensitivity[57], *At*WRKY40 was induced in response to microbial pathogen infection[58] as well as MeJA treatment[59], *At*WRKY25 was involved in plant defense against *Pseudomonas syringae*, and also acted as a cold resistance gene[60]. Another polyploidy-responsive member *Ii*WRKY50, not found integrated in the network, was designated as a calmodulin binding protein according to the protein annotation of its *Arabidopsis* ortholog *At*WRKY21. Since calcium serves as an important second messenger in plants, and changes in calcium concentration are closely related to plant responses to various stimuli[61], the expression of calcium-related proteins such as *Ii*WRKY50 might indirectly influence plant performance. To sum up, it can be conceived that, during plant development, the up-regulation of *WRKY* caused by the environmental stresses (*e.g.*, pathogen, salinity, coldness, drought, etc.) would result in higher stress tolerance, thus prompting higher growth performance (*e.g.*, higher yield and enhanced metabolites biosynthetic efficiency). Therefore, we can expect that the up-regulation of *WRKY* TFs (*IiWRKY33*, *IiWRKY34*, *IiWRKY48*, *IiWRKY49* and *IiWRKY50*) induced by autopolyploidy suggested tetraploid *I. indigotica* had a much stronger adaptation capacity than diploid progenitor.

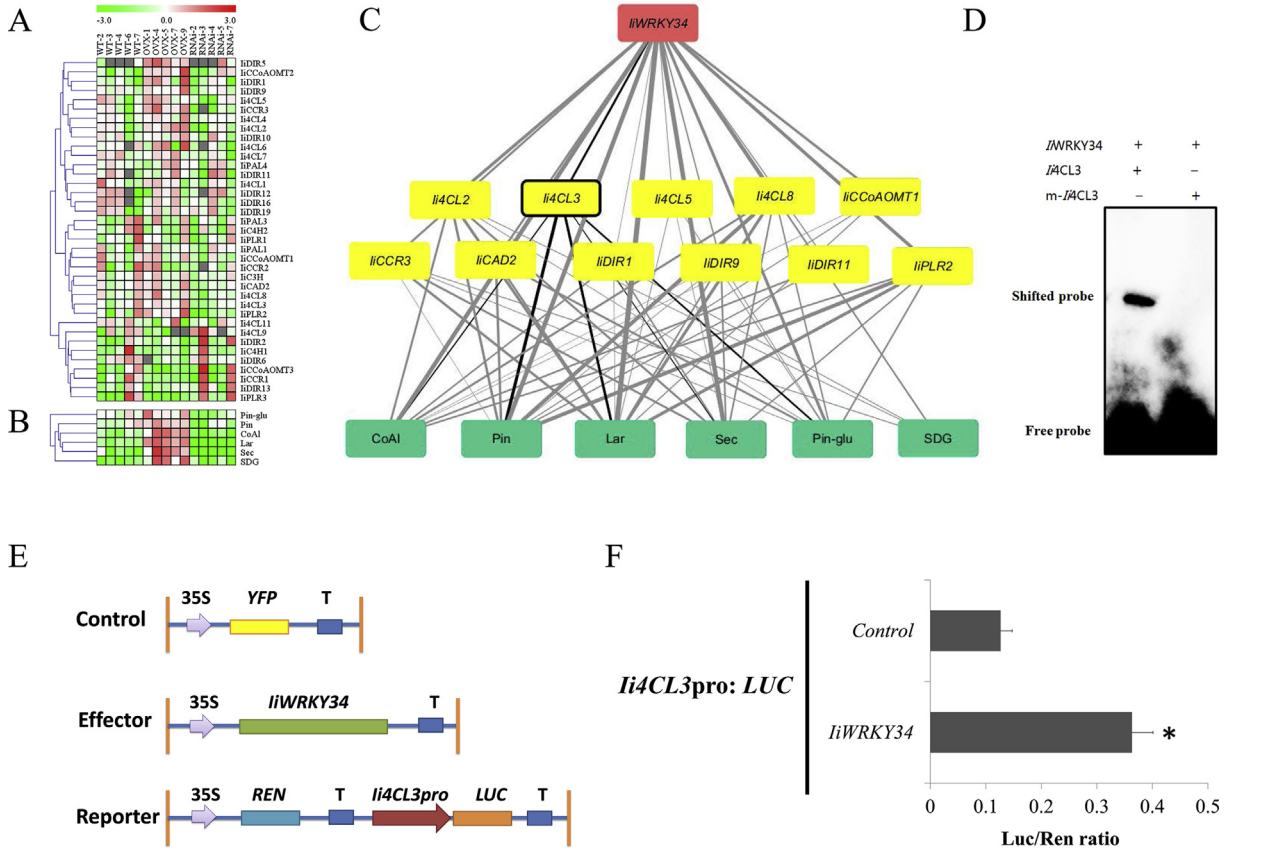

Figure 7 Regulatory network of *Ii*WRKY34 for lignan biosynthesis. Heat maps showing expression profiles of lignan biosynthetic genes (A) and lignan accumulations (B) in *IiWRKY34*-OVX, *IiWRKY34*-RNAi and WT lines. (C) *IiWRKY34*-lignan pathway genes−lignans correlation network with a cut-off $R>0.5$. *IiWRKY34*, pathway genes and lignans are drawn in red, yellow and green, respectively. The thickness of lines represents the level of correlation. *IiWRKY34*−*Ii4CL3*−lignans correlation was highlighted by black lines. (D) *Ii*WRKY34 specifically binds to the promoter of *Ii4CL3*. (E) Schematic diagram of the reporter and effector constructs used in the transient dual luciferase assay. (F) Transient dual luciferase analysis showing *Ii*WRKY34 activation of the transcription of *Ii4CL3* in *N. benthamiana* leaves. LUC/REN represents the luciferase/renilla ratio of $n=3$ independent experiments; Data were expressed as means±SD. Asterisk represents significant difference at 0.05 level by Student's *t*-test.

Paralleled with our previous report of *IiSDD1*, a gene specialized in stomatal density and distribution[12], this work implies a key advantage of "fast-evolution" by artificial breeding. Why did the polyploid become more adaptable than the diploid one? A possible mechanism is: the changed expression of critical genes, such as transcription factor *IiWRKYs* and functional gene *IiSDD1*, prompts the regulatory effect more significantly. This study proposes that WRKY not only participates in the defense/stress responses, but also associates with polyploidy vigor. The molecular mechanism of how tetraploidization leads to the expression changes of these critical genes is worth investigating in the future.

For medicinal plants, the concentration of pharmaceutical compounds is the most important factor affecting the practice of medicine[62]. Compared with diploid *I. indigotica*, the tetraploids accumulate more lignans including lariciresinol and its derivatives, which present effective antiviral ingredients of *I. indigotica*. The potency of plant-specific signaling molecules jasmonates, such as MeJA, to elicit secondary metabolism in cell cultures has made them powerful tools to cause the genetic diversity and help to unravel the complex cellular process[59]. Here, MeJA-elicited diploid and tetraploid *I. indigotica* hairy roots harvested at different time points, along with the original roots of diploid and tetraploid *I. indigotica*, were employed as a resource of genetic variation to explore the potential correlation between polyploidy-responsive *IiWRKYs* (*IiWRKY33*, *IiWRKY34*, *IiWRKY48*, *IiWRKY49* and *IiWRKY50*) and lariciresinol. Result showed *IiWRKY34* was positively correlated with lariciresinol with a high correlation coefficient value ($R = 0.812$), suggesting *Ii*WRKY34 probably participated in lariciresinol biosynthesis. Further evidence for a role of *IiWRKY34* in the regulation of secondary metabolites has been found in its orthologs from other plants. For instance, *Ga*WRKY1, also an ortholog of *At*WRKY40, regulates the production of gossypol in cotton[63]; *Cr*WRKY13, another ortholog of *At*WRKY40, is involved in biosynthesis of terpenoidindole alkaloids in *Catharanthus*[64]. Therefore, we further investigated the effect of *IiWRKY34* expression in lariciresinol biosynthesis using transgenic hairy root assays. Overexpression and RNAi analysis demonstrate that *Ii*WRKY34 is an activator of lignans including lariciresinol, and it also plays a positive role in biomass accumulation (Fig. 3), as well as salt and drought tolerance as indicated by the changes of ROS level, proline content and total antioxidant capacity of transgenic hairy roots under stress conditions (Fig. 4).

Since large alterations were observed in the developmental phenotype for *IiWRKY34*-transgenic hairy roots, their molecular phenotype was characterized by changes to both transcript and metabolism. Generally speaking, both transcriptome and metabolome profiling from individual groups (*IiWRKY34*-OVX, *IiWRKY34*-RNAi and WT hairy roots, 5 lines in each group) showed a distinct sample separation (Figs. 5A and 6A), indicating *IiWRKY34* expression made a marked effect on reshaping molecular phenotype of *I. indigotica.* Pathway classification of the DEGs revealed that *Ii*WRKY34 appeared to affect both primary and secondary metabolism, including carbon metabolism, starch and sucrose metabolism, amino acids biosynthesis and phenylpropanoid biosynthesis, etc (Fig. 5C). Measurement of metabolic shifts supported this conclusion, and *IiWRKY34* expression can drive carbon flux to specific overaccumulations of phenylpropanoids including flavonoids and lignans (Fig. 6). However, the content of the downstream compounds in the biosynthetic pathway of macrocyclopropanediol did not change significantly, suggesting *Ii*WRKY34 modulated the flux not through genetic regulation of the enzymatic steps involved in this pathway. Therefore, *Ii*WRKY34 modifications on lignan accumulations are the combined outcome of a much more complex interplay of various metabolic pathways, not merely due to the activated phenylpropanoid biosynthetic steps.

To get insight into the specific molecular mechanism of *Ii*WRKY34 for lignan biosynthesis, a *IiWRKY34*−lignan pathway genes−lignans network (Fig. 7C) was constructed based on transcript−metabolite correlation. *Ii4CL3*, which has been demonstrated as a hub gene for lignan biosynthesis, was found to be a potential target gene of *Ii*WRKY34. EMSA and dual luciferase assays demonstrated that *Ii*WRKY34 indeed activated the transcription of *Ii4CL3* by binding to the promoter (Fig. 7D and F). These results indicate that *Ii*WRKY34 modulates lignan biosynthesis, at least in part, due to regulate *Ii*4CL3, revealing the regulatory network of *Ii*WRKY34 for lignan biosynthesis is robust and the identified target genes are worthy to be intensively investigated.

5. Conclusions

Numerous genes that individually control plant growth, secondary metabolism and stress response have been identified. Compared with these genes, *Ii*WRKY34 has large pleiotropic effects on an array of traits, including yield, lignan biosynthesis and stress tolerance, which are inferred to has contributed significantly to the high level of polyploidy vigor of *I. indigotica.* Strong expression of *IiWRKY34* in tetraploid *I. indigotica* corresponded well with greater yield, higher lignan accumulation and enhanced stress tolerance of the tetraploids. The major effects of *Ii*WRKY34 will prompt the possibility of this gene based molecular marker-assisted selection and transformation for the improvement of herbs instead of individually manipulating the component traits using multiple genes of small effects.

Acknowledgments

This work was sponsored by National Natural Science Foundation of China (Grant Nos. 31872665, 81874335 and 31670292) and Shanghai Rising-Star Program (18QB1402700, China).

Author contributions

Ying Xiao, Wansheng Chen and Lei Zhang planned and designed the research. Ying Xiao, Jingxian Feng, Qing Li, Yangyun Zhou, Qitao Bu, Junhui Zhou and Hexin Tan performed experiments. Ying Xiao, Jingxian Feng, YingboYang, Wansheng Chen and Lei Zhang analysed data. Ying Xiao and Jingxian Feng wrote the manuscript. All authors read and approved the final manuscript.

Conflicts of interest

The authors have no conflicts of interest to declare.

Appendix A. Supporting information

Supporting data to this article can be found online at https://doi.org/10.1016/j.apsb.2019.12.020.

References

1. Osborn TC, Pires JC, Birchler JA, Auger DL, Chen ZJ, Lee HS, et al. Understanding mechanisms of novel gene expression in polyploids. *Trends Genet* 2003;**19**:141−7.
2. Alix K, Gérard PR, Schwarzacher T, Heslopharrison J. Polyploidy and interspecific hybridization: partners for adaptation, speciation and evolution in plants. *Ann Bot-London* 2017;**120**:183−94.
3. Cheng F, Wu J, Cai X, Liang J, Freeling M, Wang X. Gene retention, fractionation and subgenome differences in polyploid plants. *Nat Plants* 2018;**4**:258−68.
4. Council NP. *China pharmacopoeia*. 2013 ed. Beijing: Beijing Chemical Industry; 2015.
5. Li B. *Studies on active constituents and quality evaluation of Banlangen*. Shanghai: Second Military University; 2003.
6. Li J, Zhou B, Li C, Chen Q, Wang Y, Li Z, et al. Lariciresinol-4-*O*-*β*-D-glucopyranoside from the root of *Isatis indigotica* inhibits influenza A virus-induced pro-inflammatory response. *J Ethnopharmacol* 2015;**174**:379−86.
7. Yang Z, Wang Y, Zheng Z, Zhao S, Zhao J, Lin Q, et al. Antiviral activity of *Isatis indigotica* root-derived clemastanin B against human and avian influenza A and B viruses *in vitro*. *Int J Mol Med* 2013;**31**:867−73.
8. Qiao CZ. Studies on polyploid breeding of *Isatis indigotica* Fort. *J Integr* 1989;**31**:678−83.
9. Qiao C, Li H. Cultivation and popularization for tetraploidy strain of *Isatis indigotica*. *J Chin Med Mater* 1994;**17**:3−6.
10. Initiative AG. Analysis of the genome sequence of the flowering plant *Arabidopsis thaliana*. *Nature* 2000;**408**:796−815.
11. Lu B, Pan X, Zhang L, Huang B, Sun L, Li B, et al. A genome-wide comparison of genes responsive to autopolyploidy in *Isatis indigotica* using *Arabidopsis thaliana* Affymetrix genechips. *Plant Mol Biol Report* 2006;**24**:197−204.
12. Xiao Y, Yu X, Chen J, Di P, Chen W, Zhang L. *Ii*SDD1, a gene responsive to autopolyploidy and environmental factors in *Isatis indigotica*. *Mol Biol Rep* 2010;**37**:987−94.
13. Pan X, Xiao Y, Wang Z, Zhang L, Tang K. Tetraploids *Isatis indigotica* are more responsive and adaptable to stresses than the diploid progenitor based on changes in expression patterns of a cold inducible *Ii*CPK1. *Biologia* 2008;**63**:535−41.
14. Lu B, Ding R, Zhang L, Yu X, Huang B, Chen W. Molecular cloning and characterization of a novel calcium-dependent protein kinase gene *Ii*CPK2 responsive to polyploidy from tetraploid *Isatis indigotica*. *J Biochem Mol Biol* 2006;**39**:607−17.
15. Lu B, Du Z, Ding R, Zhang L, Yu X, Liu C, et al. Cloning and characterization of a differentially expressed phenylalanine ammonialyase gene (*li*PAL) after genome duplication from tetraploid *Isatis indigotica* Fort. *J Integr* 2006;**48**:1439−49.
16. Zhou Y, Kang L, Liao S, Pan Q, Ge X, Li Z. Transcriptomic analysis reveals differential gene expressions for cell growth and functional secondary metabolites in induced autotetraploid of Chinese Woad (*Isatis indigotica* Fort.). *PLoS One* 2015;**10**:e116392.
17. Colinas M, Goossens A. Combinatorial transcriptional control of plant specialized metabolism. *Trends Plant Sci* 2018;**17**:S1360−85.
18. Chu Y, Xiao S, Su H, Liao B, Zhang J, Xu J, et al. Genome-wide characterization and analysis of bHLH transcription factors in *Panax ginseng*. *Acta Pharm Sin B* 2018;**8**:666−77.
19. Zhang Y, Xu Z, Ji A, Luo H, Song J. Genomic survey of bZIP transcription factor genes related to tanshinone biosynthesis in *Salvia miltiorrhiza*. *Acta Pharm Sin B* 2018;**8**:295−305.
20. Chen F, Hu Y, Vannozzi A, Wu K, Cai H, Qin Y, et al. The WRKY transcription factor family in model plants and crops. *Crit Rev Plant Sci* 2018;**36**:1−25.
21. Chen J, Xin D, Li Q, Xun Z, Gao S, Chen R, et al. Biosynthesis of the active compounds of *Isatis indigotica* based on transcriptome sequencing and metabolites profiling. *BMC Genomics* 2013;**14**:857.
22. Altschul SF, Madden TL, Schäffer AA, Zhang J, Zhang Z, Miller W, et al. Gapped BLAST and PSI-BLAST: a new generation of protein database search programs. *Nucleic Acids Res* 1997;**25**:3389−402.
23. Punta M, Coggill PC, Eberhardt RY, Mistry J, Tate J, Boursnell C, et al. The Pfam protein families database. *Nucleic Acids Res* 2004;**28**:263−6.
24. Schultz J, Milpetz F, Bork P, Ponting CP. SMART, a simple modular architecture research tool: identification of signaling domains. *Proc Natl Acad Sci U S A* 1998;**95**:5857−64.
25. Letunic I, Doerks T, Bork P. Smart 7: recent updates to the protein domain annotation resource. *Nucleic Acids Res* 2012;**40**:302−5.
26. Gasteiger E, Hoogland C, Gattiker A, Duvaud S, Wilkins MR, Appel RD, et al. Protein identification and analysis tools on the ExPASy server. *Methods Mol Biol* 1999;**112**:531.
27. Larkin MA, Blackshields G, Brown NP, Chenna R, Mcgettigan PA, Mcwilliam H, et al. Clustal W and clustal X version 2.0. *Bioinformatics* 2007;**23**:2947−8.
28. Tamura K, Peterson D, Peterson N, Stecher G, Nei M, Kumar S. MEGA5: molecular evolutionary genetics analysis using maximum likelihood, evolutionary distance, and maximum parsimony methods. *Mol Biol Evol* 2011;**28**:2731−9.
29. Eulgem T, Rushton PJ, Robatzek S, Somssich IE. The WRKY superfamily of plant transcription factor. *Trends Plant Sci* 2000;**5**:199−206.
30. Bailey TL, Boden M, Buske FA, Frith M, Grant CE, Clementi L, et al. Meme suite: tools for motif discovery and searching. *Nucleic Acids Res* 2009;**37**:W202−8.
31. Szklarczyk D, Franceschini A, Kuhn M, Simonovic M, Roth A, Minguez P, et al. The STRING database in 2011: functional interaction networks of proteins, globally integrated and scored. *Nucleic Acids Res* 2010;**39**:D561−8.
32. Li Q, Chen J, Xiao Y, Di P, Zhang L, Chen W. The dirigent multigene family in *Isatis indigotica*: gene discovery and differential transcript abundance. *BMC Genomics* 2014;**15**:388.
33. Xiao Y, Ji Q, Gao S, Tan H, Chen R, Li Q, et al. Combined transcriptome and metabolite profiling reveals that *Ii*PLR1 plays an important role in lariciresinol accumulation in *Isatis indigotica*. *J Exp Bot* 2015;**66**:6259.
34. Saito K, Matsuda F. Metabolomics for functional genomics, systems biology, and biotechnology. *Annu Rev Plant Biol* 2010;**61**:463−89.
35. Wesley SV, Helliwell CA, Smith NA, Wang MB, Rouse DT, Liu Q, et al. Construct design for efficient, effective and high-throughput gene silencing in plants. *Plant J* 2001;**27**:581−90.
36. Chilton MD, Tepfer DA, Petit A, David C, Cassedelbart F, Tempé J. *Agrobacterium rhizogenes* inserts T-DNA into the genomes of the host plant root cells. *Nature* 1982;**295**:432−4.
37. de Micco V, Aronne G. Combined histochemistry and autofluorescence for identifying lignin distribution in cell walls. *Biotech Histochem* 2007;**82**:209−16.
38. Wang F, Chen HW, Li QT, Wei W, Li W, Zhang WK, et al. *Gm*WRKY27 interacts with *Gm*MYB174 to reduce expression of *Gm*NAC29 for stress tolerance in soybean plants. *Plant J* 2015;**83**:224−36.
39. Bates LS, Waldren RP, Teare ID. Rapid determination of free proline for water-stress studies. *Plant Soil* 1973;**39**:205−7.
40. Zhang Y, Yan YP, Wang ZZ. The *Arabidopsis* PAP1 transcription factor plays an important role in the enrichment of phenolic acids in *Salvia miltiorrhiza*. *J Agric Food Chem* 2010;**58**:12168−75.
41. Consortium TGO, Ashburner M, Ball CA, Blake JA, Botstein D, Butler H, et al. Gene ontology: tool for the unification of biology. *Nat Genet* 2000;**25**:25−9.
42. Draghici S, Khatri P, Tarca AL, Amin K, Done A, Voichita C, et al. A systems biology approach for pathway level analysis. *Genome Res* 2007;**17**:1537.
43. Lisec J, Schauer N, Kopka J, Willmitzer L, Fernie AR. Gas chromatography mass spectrometry-based metabolite profiling in plants. *Nat Protoc* 2006;**1**:387−96.

44. Saeed AI, Sharov V, White J, Li J, Liang W, Bhagabati N, et al. TM4: a free, open-source system for microarray data management and analysis. *Biotechniques* 2003;**34**:374−8.
45. Cline MS, Smoot M, Cerami E, Kuchinsky A, Landys N, Workman C, et al. Integration of biological networks and gene expression data using cytoscape. *Nat Protoc* 2007;**2**:2366−82.
46. Zhang F, Fu X, Lv Z, Lu X, Shen Q, Zhang L, et al. A basic leucine zipper transcription factor, *Aa*bZIP1, connects abscisic acid signaling with artemisinin biosynthesis in *Artemisia annua*. *Mol Plant* 2015;**8**: 163−75.
47. Yamasaki K, Kigawa T, Inoue M, Tateno M, Yamasaki T, Yabuki T, et al. Solution structure of an *Arabidopsis* WRKY DNA binding domain. *Plant Cell* 2005;**17**:944−56.
48. Guo C, Guo R, Xu X, Gao M, Li X, Song J, et al. Evolution and expression analysis of the grape (*Vitis vinifera* L.) WRKY gene family. *J Exp Bot* 2014;**65**:1513−28.
49. He H, Dong Q, Shao Y, Jiang H, Zhu S, Cheng B, et al. Genome-wide survey and characterization of the gene family in *Populus trichocarpa*. *Plant Cell Rep* 2012;**31**:1199−217.
50. Ling J, Jiang W, Zhang Y, Yu H, Mao Z, Gu X, et al. Genome-wide analysis of WRKY gene family in *Cucumis sativus*. *BMC Genomics* 2011;**12**:471.
51. Sakamoto H, Maruyama K, Sakuma Y, Meshi T, Iwabuchi M, Shinozaki K, et al. *Arabidopsis* Cys2/His2-type zinc-finger proteins function as transcription repressors under drought, cold, and high-salinity stress conditions. *Plant Physiol* 2004;**136**:2734−46.
52. Zhou C, Zhang L, Duan J, Miki B, Wu K. Histone deacetylase19 is involved in jasmonic acid and ethylene signaling of pathogen response in *Arabidopsis*. *Plant Cell* 2005;**17**:1196−204.
53. Xie Y, LI W, Guo D, Dong J, Zhang Q, Fu Y, et al. The *Arabidopsis* gene sigma factor-binding protein 1 plays a role in the salicylate- and jasmonate-mediated defence responses. *Plant Cell Environ* 2010;**33**: 828−39.
54. Hano C, Addi M, Bensaddek L, Crã Nier D, Baltora-Rosset S, Doussot J, et al. Differential accumulation of monolignol-derived compounds in elicited flax (*Linum usitatissimum*) cell suspension cultures. *Planta* 2006;**223**:975−89.
55. Ashraf M, Foolad MR. Roles of glycine betaine and proline in improving plant abiotic stress resistance. *Environ Exp Bot* 2007;**59**: 206−16.
56. Zhang L, Chen J, Zhou X, Chen X, Li Q, Tan H, et al. Dynamic metabolic and transcriptomic profiling of methyl jasmonate-treated hairy roots reveals synthetic characters and regulators of lignan biosynthesis in *Isatis indigotica* Fort. *Plant Biotechnol J* 2016;**14**:2217−27.
57. Jiang Y, Deyholos MK. Functional characterization of Arabidopsis NaCl-inducible WRKY25 and WRKY33 transcription factors in abiotic stresses. *Plant Mol Biol* 2009;**69**:91−105.
58. Rushton DL, Tripathi P, Rabara RC, Lin J, Ringler P, Boken AK, et al. WRKY transcription factors: key components in abscisic acid signalling. *Plant Biotechnol J* 2011;**10**:2−11.
59. Pauwels L, Morreel K, Witte ED, Lammertyn F, Montagu MV, Boerjan W, et al. Mapping methyl jasmonate-mediated transcriptional reprogramming of metabolism and cell cycle progression in cultured *Arabidopsis* cells. *P Natl Acad Sci USA* 2008;**105**:1380−5.
60. Zheng Z, Mosher SL, Fan B, Klessig DF, Chen Z. Functional analysis of *Arabidopsis* WRKY25 transcription factor in plant defense against *Pseudomonas syringae*. *BMC Plant Biol* 2007;**7**:2.
61. Bush DS. Calcium regulation in plant cells and its role in signaling. *Annu Rev Plant Physiol Plant Mol Biol* 1995;**46**:95−122.
62. Gechev TS, Hille J, Woerdenbag HJ, Benina M, Mehterov N, Toneva V, et al. Natural products from resurrection plants: potential for medical applications. *Biotechnol Adv* 2014;**32**:1091−101.
63. Xu Y, Wang J, Wang S, Wang J, Chen X. Characterization of *Ga*WRKY1, a cotton transcription factor that regulates the sesquiterpene synthase gene (+)-*δ*-cadinene synthase-A. *Plant Physiol* 2004; **135**:507−15.
64. Schluttenhofer C, Pattanaik S, Patra B, Yuan L. Analyses of *Catharanthus roseus* and *Arabidopsis thaliana* WRKY transcription factors reveal involvement in jasmonate signaling. *BMC Genomics* 2014;**15**: 502.